Modelling Grain Growth in the Framework of Rational Extended Thermodynamics

Lukas Kertsch, Dirk Helm

Fraunhofer Institute for Mechanics of Materials IWM
Wöhlerstraße 11, 79108 Freiburg, Germany

E-mail: lukas.kertsch@iwm.fraunhofer.de

Abstract. Grain growth is a significant phenomenon for the thermomechanical processing of metals. Since the mobility of the grain boundaries is thermally activated and energy stored in the grain boundaries is released during their motion, a mutual interaction with the process conditions occurs. To model such phenomena, a thermodynamic framework for the representation of thermomechanical coupling phenomena in metals including a microstructure description is required. For this purpose, Rational Extended Thermodynamics appears to be a useful tool. We apply an entropy principle to derive a thermodynamically consistent model for grain coarsening due to the growth and shrinkage of individual grains. Despite the rather different approaches applied, we obtain a grain growth model which is similar to existing ones and can be regarded as a thermodynamic extension of that by Hillert (1965) to more general systems. To demonstrate the applicability of the model, we compare our simulation results to grain growth experiments in pure copper by different authors, which we are able to reproduce very accurately. Finally, we study the implications of the energy release due to grain growth on the energy balance. The present unified approach combining a microstructure description and continuum mechanics is ready to be further used to develop more elaborate material models for complex thermo-chemo-mechanical coupling phenomena.

PACS numbers: 05.70, 46.15, 62.20, 65.40, 68.35, 81.05, 81.10

Keywords: Constitutive Modelling, Thermodynamic Modelling, Grain Growth, Microstructure, Metallic Materials, Thermomechanical Processing Submitted to:

Modelling Simul. Mater. Sci. Eng.

1. Introduction

The thermal, mechanical and chemical properties of metals are strongly coupled by their microstructure. This knowledge is used for designing appropriate thermomechanical process chains to obtain a large variety of material states with different properties. For the predictive power of a material model used in such processes it is therefore

crucial to take the strong thermomechanical coupling and the underlying microstructure behaviour into account. In order to ensure that all constitutive relations are consistent and physically meaningful, the models should be derived out of a thermodynamic framework. In the following, we briefly review some thermodynamic concepts for irreversible processes to provide a basis for our subsequent analysis.

In Irreversible Thermodynamics, generalised thermodynamic forces and fluxes are introduced outside equilibrium, whose respective products contribute to the entropy production rate [1]. Generally, all forces and fluxes are interrelated with each other. If this relation is linearised, it can be expressed in terms of phenomenological coefficients, for which Onsager suggested reciprocal relations [2, 3]. Furthermore, based on the dissipation potential, Onsager formulated an extremal principle to determine the evolution of a thermodynamic system. However, these considerations have been controversially discussed [4].

For application in continuum mechanics, Rational Thermodynamics developed by Coleman and Noll [5] is frequently used. Following this concept, only those constitutive equations are admissible whose general structure comply with the second law of thermodynamics in terms of the Clausius-Duhem inequality. Being very advantageous for thermomechanically coupled problems, the concept contains some critical aspects, though. The entropy flux is postulated a priori as the heat flux divided by the temperature, a result valid only in the vicinity of equilibrium [1]. In addition, a volume-distributed heat production term, referred to as "radiation", is introduced in the energy balance, which, divided by the temperature, recurs as an entropy source density. Appropriate body forces and radiation must be applied to fulfil the balance equations for admissible thermodynamic processes. Moreover, the principle is not intended for the use of internal variables with constraints.

These drawbacks are eliminated by various approaches referred to Rational Extended Thermodynamics [6]. The entropy principle formulated by Müller does not require an a priori assumption of the entropy flux but leaves it as a constitutive quantity [7]. The method of Lagrange multipliers developed by Liu allows to consider all conservation laws of continuum mechanics and additional constraints as side conditions to the entropy inequality [8]. As a consequence, the heat source density and body forces are no longer needed to fulfil the balance equations but they can be controlled by the environment. Liu used the example of a simple heat conducting fluid to demonstrate the general applicability of his principle [8]. This treatment has been extended by Müller to a mixture of fluids with several additional features [9] and by Svendsen and Hutter to more general mixtures of viscous media [10]. However, to our knowledge most examples in literature using Liu's principle rather focus on theoretical aspects than on practical application.

As a first step towards incorporating the microstructure into a coupled material model, in the present work we set up a simplified grain structure description. The thermodynamic principle applied then directly implies an associated model for grain growth. Strictly speaking, this phenomenon should be addressed as grain coarsening

because the global effect is the result of the growth of larger grains and shrinkage of smaller ones. Due to the more frequent usage in literature, however, we use the term growth as a synonym for coarsening.

Early empirical mean-field descriptions of grain growth have been developed by Burke and Turnbull [11] and others, who derived evolution equations for the mean grain size in a system. Denoting the mean radius by $\overline{r}$, they proposed the relation

$$\overline{r}^2 - \overline{r}_0^2 = A\sigma t, \tag{1}$$

where $\overline{r}_0$ is the initial mean radius, A is a constant, σ denotes the grain boundary energy per unit area and t time. This equation is still often used as a first approximation to describe experimental results. However, the predictive power of (1) is limited because only the mean size is considered.

Based on the works by Feltham [12], von Neumann [13], Mullins [14] and Lifshitz and Slyozov [15], Hillert [16] derived a growth equation for individual grains. In our notation, for one grain α he obtained the relation

$$\dot{r}_\alpha = cM\sigma \left(\frac{1}{r_{\mathrm{cr}}} - \frac{1}{r_\alpha} \right), \tag{2}$$

for the evolution of its radius. In this equation, M is the grain boundary mobility and r_{cr} the critical radius above which a grain grows and below which it shrinks. For two-dimensional problems, Hillert identified the critical radius as the arithmetic mean radius, $r_{\mathrm{cr}} = \overline{r}$, and found $c = 1/2$. In three dimensions, he obtained $r_{\mathrm{cr}} = 9/8\ \overline{r}$ and $c = 1$. Although this model is able to express the evolution of individual grains, it is a mean-field approach in that the microstructure is not spatially resolved and the grains are simplified as spherical objects. For normal grain growth, this theory results in a unique distribution of grain sizes.

Rios and Glicksman used the concept of "average N-hedra", a way to statistically describe the characteristics of an irregular grain network, to study the influence of the grain topology. They were able to reproduce Hillert's grain size distribution in two [17] and three dimensions[18] by applying simplifying assumptions on the topology.

Increasing computational capabilities gave rise to the development of full-field models for a spatially resolved microstructure description. Full-field grain growth models have been developed by the Monte Carlo method [19, 20], vertex dynamics [21], the surface evolver method [22], cellular automata [23, 24] and the phase-field method [25, 26]. Especially phase-field models allow detailed simulations with very efficient codes [27]. There is concurrent evidence from several full-field models, e. g. [22, 26], that taking the topology into account, the steady-state grain size distribution slightly deviates from Hillert's prediction. On the other hand, Darvishi Kamachali and Steinbach [28] showed that Hillert's solution is not unique and that by an alternative treatment, the mean-field and full-field predictions can be reconciled.

In this work, however, we use a mean-field approach without topological information having a further utilisation of the microstructure model within a unified continuum thermo-chemo-mechanical model in mind. For this purpose, we are rather interested in

an efficient method to obtain approximate information about the microstructure than in an accurate description of its details. There are already many strategies available to describe coupled phenomena on the microstructure level by mean-field models like the impact of the Zener drag due to particles on grain growth [29]. Rios et al. showed that the Zener force can be treated within the framework of Irreversible Thermodynamics [30]. However, most models are not developed from a thermodynamic framework.

For the particular case of pure grain growth, Berdichevsky formulated a variational approach to investigate entropy effects [31], explicitly referring to Hillert [16]. Fischer et al. employed Onsager's extremal principle from Irreversible Thermodynamics, [2, 3], and obtained

$$\dot{r}_\alpha = cM_\alpha\sigma_\alpha\left(\frac{1}{r_{\mathrm{cr},\alpha}} - \frac{1}{r_\alpha}\right), \tag{3}$$

for an ensemble of N individual grains [32]. This result reveals a strong similarity to Hillert's theory but allows the treatment of more general cases. For two-dimensional systems, the parameters are $c = 1$ and

$$r_{\mathrm{cr},\alpha} = \frac{\sum_{\beta=1}^{N} M_\beta r_\beta}{\sum_{\beta=1}^{N} M_\beta \frac{\sigma_\beta}{\sigma_\alpha}}, \tag{4}$$

whereas for three-dimensional systems $c = 2$ and

$$r_{\mathrm{cr},\alpha} = \frac{\sum_{\beta=1}^{N} M_\beta r_\beta^2}{\sum_{\beta=1}^{N} M_\beta \frac{\sigma_\beta}{\sigma_\alpha} r_\beta}. \tag{5}$$

In the present work, we apply the concept of Rational Extended Thermodynamics because it offers both a rigorous framework for establishing thermodynamic consistency between all relevant thermomechanical quantities and the flexibility to handle additional constraints related to the microstructure model. In our future work, we intend to exploit this potential by including various fields and variables in the model. Therefore, we select a very simple microstructure description being aware that the resulting model only represents a rough estimation. The paper is structured as follows: In section 2, we outline the thermodynamic framework for the subsequent analysis from general balance equations to an entropy principle. In section 3, we incorporate a microstructure model into the continuum framework and derive a grain growth model. In section 4, we discuss our model and compare it to existing ones. We present numerical results from the application to grain growth in pure copper and analyse the implications on the energy balance.

2. Thermodynamic Framework

2.1. Balance Equations and Constitutive Assumptions

The classical conservation laws in continuum mechanics are the mass balance,

$$\dot{\rho} + \rho \operatorname{div} \boldsymbol{v} = 0, \tag{6}$$

the balance of linear momentum,

$$\rho\dot{\boldsymbol{v}} = \operatorname{div}\mathbf{T} + \rho\boldsymbol{f}, \tag{7}$$

and the energy balance or first law of thermodynamics,

$$\rho\dot{e} + \frac{1}{2}\rho\left(\boldsymbol{v}\cdot\boldsymbol{v}\right)^{\cdot} = \operatorname{div}\left(\mathbf{T}^{\mathsf{T}}\boldsymbol{v}\right) + \rho\boldsymbol{f}\cdot\boldsymbol{v} - \operatorname{div}\boldsymbol{q}. \tag{8}$$

In the above equations, ρ denotes the mass density, $\boldsymbol{v}$ the velocity, $\mathbf{T}$ the Cauchy stress tensor, $\boldsymbol{f}$ a specific body force, e the specific internal energy and $\boldsymbol{q}$ the heat flux vector. The dot $(\cdot)^{\cdot}$ denotes the material derivative. Note that no heat source density is considered in the energy balance. It is not required for thermodynamic consistency and we exclude the case that heat is supplied by fields. Assuming that there exists an absolute temperature θ, it is convenient to use the Helmholtz free energy

$$\psi = e - \theta\eta \tag{9}$$

as a thermodynamic potential instead of the internal energy. In (9), η denotes the specific entropy.

Thermodynamic consistency requires further that the second law of thermodynamics, or the principle of irreversibility, is fulfilled, which postulates a non-negative entropy production γ for every admissible thermodynamic process. The entropy production is the sum of the change within the volume and the flux $\boldsymbol{\phi}$ across the surface, which can locally be expressed as

$$\rho\gamma = \rho\dot{\eta} + \operatorname{div}\boldsymbol{\phi} \geq 0. \tag{10}$$

Therefore, the entropy balance is not a conservation law. Following the ideas of Müller [7], no a priori constitutive assumption for $\boldsymbol{\phi}$ is made nor is a volume-distributed entropy supply introduced, which is motivated by the absence of any volume-distributed energy supply.

We use internal state variables to express the process history and to model the microstructure [33]. The internal variables may, in turn, be subdivided into multiple sets. If there are variables whose evolution is subject to side conditions, we distinguish S sets $\left\{q_{\alpha_\xi}\right\}$ $(\alpha_\xi = 1,\ldots,N_\xi)$ and denote the respective side conditions by

$$f_\xi\left(\left\{q_{\alpha_\xi}\right\},\left\{\dot{q}_{\alpha_\xi}\right\},\ldots\right) = 0 \quad (\xi = 1,\ldots,S) \tag{11}$$

which generally might depend on further arguments than $\left\{q_{\alpha_\xi}\right\}$ and its derivative. The last set of internal variables, $\{q_\beta\}$ $(\beta = 1,\ldots,M)$, comprises those which are not restricted by further conditions.

For the quantities ψ, η, $\mathbf{T}$, $\boldsymbol{q}$ and $\boldsymbol{\phi}$, constitutive relations are needed. We assume that they may depend on the deformation gradient $\mathbf{F}$, temperature θ and $\boldsymbol{g} = \operatorname{grad}\theta$ as well as on the internal variable sets $\left\{q_{\alpha_\xi}\right\}$ and $\{q_\beta\}$. The principle of equipresence states that all constitutive equations should depend on the same set of independent variables [34]. Consequently, the general forms of the constitutive equations are

$$\psi = \hat{\psi}(\mathbf{F},\theta,\boldsymbol{g},\left\{q_{\alpha_\xi}\right\},\{q_\beta\}), \tag{12}$$

$$\eta = \hat{\eta}(\mathbf{F},\theta,\boldsymbol{g},\left\{q_{\alpha_\xi}\right\},\{q_\beta\}), \tag{13}$$

$$\mathbf{T} = \hat{\mathbf{T}}(\mathbf{F}, \theta, \boldsymbol{g}, \left\{q_{\alpha_\xi}\right\}, \{q_\beta\}), \tag{14}$$

$$\boldsymbol{q} = \hat{\boldsymbol{q}}(\mathbf{F}, \theta, \boldsymbol{g}, \left\{q_{\alpha_\xi}\right\}, \{q_\beta\}), \tag{15}$$

$$\boldsymbol{\phi} = \hat{\boldsymbol{\phi}}(\mathbf{F}, \theta, \boldsymbol{g}, \left\{q_{\alpha_\xi}\right\}, \{q_\beta\}). \tag{16}$$

In addition, evolution equations for $\left\{q_{\alpha_\xi}\right\}$ and $\{q_\beta\}$ are needed.

2.2. Entropy Principle

In order to find admissible expressions for the constitutive quantities, the second law has to be evaluated taking all balances and restrictions from section 2.1 into account. Liu showed that field equations which are linear in the highest derivatives of the fields can be used as side conditions to the entropy inequality and may be appended to the inequality by means of Lagrange multipliers [8]. This condition holds for the balance equations (6), (7) and (8). If the restrictions on the internal variables, (11), are linear in the highest derivatives, too, we may supplement the inequality (10) by all these equations and obtain the condition that

$$\begin{aligned}
\rho\gamma = {} & \rho\dot{\eta} + \operatorname{div}\boldsymbol{\phi} \\
& - \lambda^\rho \left\{\dot{\rho} + \rho \operatorname{div}\boldsymbol{v}\right\} \\
& - \boldsymbol{\lambda}^{\boldsymbol{v}} \cdot \left\{\rho\dot{\boldsymbol{v}} - \operatorname{div}\mathbf{T} - \rho\boldsymbol{f}\right\} \\
& - \lambda^e \Big\{\rho\dot{\psi} + \rho\theta\dot{\eta} + \rho\eta\dot{\theta} + \rho\boldsymbol{v}\cdot\dot{\boldsymbol{v}} - \operatorname{div}(\mathbf{T})\cdot\boldsymbol{v} - \mathbf{T}\cdot\mathbf{D} - \rho\boldsymbol{f}\cdot\boldsymbol{v} + \operatorname{div}\boldsymbol{q}\Big\} \\
& - \sum_{\xi=1}^{S} \lambda_\xi f_\xi \left(\left\{q_{\alpha_\xi}\right\}, \left\{\dot{q}_{\alpha_\xi}\right\}, \ldots\right) \geq 0
\end{aligned} \tag{17}$$

must hold for every admissible thermodynamic process. Due to the symmetry of the stress tensor, we only have to keep its product with the symmetric part $\mathbf{D}$ of the velocity gradient. The parameters λ^ρ, $\boldsymbol{\lambda}^{\boldsymbol{v}}$, λ^e and $\{\lambda_\xi\}$ are the Lagrange multipliers, which have to be determined in addition to the constitutive quantities.

Inserting the constitutive equations (12)–(16) into the inequality (17) and using the chain rule as well as the identity $\operatorname{grad}\boldsymbol{v} = \dot{\mathbf{F}}\mathbf{F}^{-1}$ provides an inequality which is linear in the derivatives

$$\dot{\mathbf{F}},\ \dot{\theta},\ \dot{\boldsymbol{g}},\ \dot{\boldsymbol{v}},\ \dot{\rho},\ \operatorname{grad}\mathbf{F},\ \operatorname{grad}\boldsymbol{g},\ \left\{\operatorname{grad} q_{\alpha_\xi}\right\},\ \left\{\operatorname{grad} q_\beta\right\}. \tag{18}$$

This inequality must hold for arbitrary values of these derivatives in order that every conceivable thermodynamic process can be realised. Therefore, the respective coefficients must vanish. As a consequence, we obtain precise constraints for the choice of the constitutive equations for ψ, η, $\mathbf{T}$, $\boldsymbol{q}$ and $\boldsymbol{\phi}$ as well as information about the Lagrange multipliers.

The residual inequality is linear in the derivatives

$$\left\{\dot{q}_{\alpha_\xi}\right\},\ \left\{\dot{q}_\beta\right\},\ \boldsymbol{g} = \operatorname{grad}\theta. \tag{19}$$

As their values are independent, we conclude that the product of each of these derivatives and their respective coefficients must be positive in order that the inequality is always

fulfilled. These conditions motivate the choice of the evolution equations for the internal variables and provide an additional constraint for the heat and entropy flux vectors.

At this point, we emphasise that besides the kinematic variables and temperature, an arbitrary number of internal variables may occur in the inequality (17), such as dislocation density, grain and second phase particle sizes, chemical composition and crystal orientation. Consequently, the set of constitutive equations, whose structure is given by the entropy principle, will be strongly coupled. While finding an appropriate solution strategy will be challenging, such couplings are in principle desired. In fact, using reasonable variables should lead to physically meaningful interrelations among each other.

3. Grain Growth Model

3.1. Microstructure Model and Evaluation of the Entropy Principle

The procedure described in section 2.2 provides information about the complete set of thermomechanical constitutive equations. In this section, we will demonstrate the suitability of this particular formulation of the entropy principle for coupled processes by incorporating a microstructure description into the material model. For simplicity, we exclude any deformation and neglect the influence of stress. Consequently, $\mathbf{T}$ and the derivatives of $\boldsymbol{v}$ vanish and we may ignore the momentum balance. The energy balance reduces to

$$\rho\dot{e} + \operatorname{div}\boldsymbol{q} = 0. \tag{20}$$

The reduced mass balance $\dot{\rho} = 0$ is trivial and has thus not to be further considered.

At each material point, we introduce a microstructure model acting on a level subordinate to the "macroscopic" world. We treat the microstructure as a representative but spatially not resolved ensemble of grains. Therefore, we approximate the grains by spheres with radii $\{r_\alpha\}$ although in the strict sense, it is impossible to completely fill a simply connected domain by such bodies. In addition, we assign the same temperature to all grains, whereas the temperature may be inhomogeneously distributed within the "macroscopic" system. The total system volume V is the sum of all individual grain volumes $V_\alpha = 4/3\,\pi r_\alpha^3$ $(\alpha = 1, \ldots, N)$ and remains constant during grain coarsening. Therefore, the condition

$$\dot{V} = \sum_{\alpha=1}^{N} \dot{V}_\alpha = 4\pi \sum_{\alpha=1}^{N} r_\alpha^2 \dot{r}_\alpha = \sum_{\alpha=1}^{N} A_\alpha \dot{r}_\alpha = 0 \tag{21}$$

has to be fulfilled, where $A_\alpha = 4\pi r_\alpha^2$ is the surface area of grain α. In the case that grain growth in a thin film leads to grain sizes of the magnitude of the film thickness h or larger, the assumption of spherical grains is no longer reasonable. Instead, each grain is approximated by a cylinder with radius r_α and height h. If A_α denotes its curved

surface area, $A_\alpha = 2\pi r_\alpha h$, (21) is still valid:

$$\dot{V} = \sum_{\alpha=1}^{N} \dot{V}_\alpha = 2\pi h \sum_{\alpha=1}^{N} r_\alpha \dot{r}_\alpha = \sum_{\alpha=1}^{N} A_\alpha \dot{r}_\alpha = 0. \tag{22}$$

The grain radii are treated as a set of internal variables constrained by (21) which will be incorporated into the entropy inequality by a Lagrange multiplier λ^V. No additional internal variables $\{q_\beta\}$ are considered at the moment.

Hence, the entropy inequality becomes

$$\rho\gamma = \rho\dot{\eta} + \operatorname{div}\boldsymbol{\phi} - \lambda^e \left\{ \rho\dot{\psi} + \rho\theta\dot{\eta} + \rho\eta\dot{\theta} + \operatorname{div}\boldsymbol{q} \right\} - \lambda^V \sum_{\alpha=1}^{N} A_\alpha \dot{r}_\alpha \geq 0. \tag{23}$$

According to the chain rule, the material derivative of the scalars $y = \{\psi, \eta\}$ and the divergence of the vectors $\boldsymbol{y} = \{\boldsymbol{q}, \boldsymbol{\phi}\}$ are

$$\dot{y} = \frac{\partial y}{\partial \theta}\dot{\theta} + \frac{\partial y}{\partial \boldsymbol{g}} \cdot \dot{\boldsymbol{g}} + \sum_{\alpha=1}^{N} \frac{\partial y}{\partial r_\alpha}\dot{r}_\alpha, \tag{24}$$

$$\operatorname{div}\boldsymbol{y} = \frac{\partial \boldsymbol{y}}{\partial \theta} \cdot \boldsymbol{g} + \frac{\partial \boldsymbol{y}}{\partial \boldsymbol{g}} \cdot \operatorname{grad}\boldsymbol{g} + \sum_{\alpha=1}^{N} \frac{\partial \boldsymbol{y}}{\partial r_\alpha} \cdot \operatorname{grad} r_\alpha. \tag{25}$$

Inserting into (23), resorting with respect to the derivatives $\dot{\theta}$, $\dot{\boldsymbol{g}}$, $\operatorname{grad}\boldsymbol{g}$, $\{\operatorname{grad} r_\alpha\}$, $\{\dot{r}_\alpha\}$ and $\boldsymbol{g}$ and following the argument from section 2.2 (a non-negative entropy production must be assured for arbitrary values of these derivatives) yields the conditions

$$\frac{\partial \eta}{\partial \theta} - \lambda^e \left(\frac{\partial \psi}{\partial \theta} + \theta \frac{\partial \eta}{\partial \theta} + \eta \right) = 0, \tag{26}$$

$$\frac{\partial \eta}{\partial \boldsymbol{g}} - \lambda^e \left(\frac{\partial \psi}{\partial \boldsymbol{g}} + \theta \frac{\partial \eta}{\partial \boldsymbol{g}} \right) = \boldsymbol{0}, \tag{27}$$

$$\frac{\partial \boldsymbol{\phi}}{\partial \boldsymbol{g}} - \lambda^e \frac{\partial \boldsymbol{q}}{\partial \boldsymbol{g}} = \boldsymbol{0}, \tag{28}$$

$$\frac{\partial \boldsymbol{\phi}}{\partial r_\alpha} - \lambda^e \frac{\partial \boldsymbol{q}}{\partial r_\alpha} = \boldsymbol{0}, \quad (\alpha = 1, \ldots, N) \tag{29}$$

$$\left\{ \rho \left[\frac{\partial \eta}{\partial r_\alpha} - \lambda^e \left(\frac{\partial \psi}{\partial r_\alpha} + \theta \frac{\partial \eta}{\partial r_\alpha} \right) \right] - \lambda^V A_\alpha \right\} \dot{r}_\alpha \geq 0, \quad (\alpha = 1, \ldots, N) \tag{30}$$

$$\left\{ \frac{\partial \boldsymbol{\phi}}{\partial \theta} - \lambda^e \frac{\partial \boldsymbol{q}}{\partial \theta} \right\} \cdot \boldsymbol{g} \geq 0. \tag{31}$$

We adopt the argument of Müller that the Lagrange multiplier of the energy balance equals the inverse absolute temperature, $\lambda^e = 1/\theta$ [7, 9], such that (26) provides the usual potential relation for the entropy,

$$\eta = -\frac{\partial \psi}{\partial \theta}, \tag{32}$$

and (27) simplifies to the statement that the free energy must not depend on the temperature gradient. This result is consistent with the usual assumptions. Consequently, the general form of the free energy for our grain coarsening model is $\psi = \hat{\psi}(\theta, \{r_\alpha\})$.

The conditions (28), (29) and (31) take the forms

$$\frac{\partial \boldsymbol{\phi}}{\partial \boldsymbol{g}} = \frac{1}{\theta}\frac{\partial \boldsymbol{q}}{\partial \boldsymbol{g}}, \tag{33}$$

$$\frac{\partial \boldsymbol{\phi}}{\partial r_\alpha} = \frac{1}{\theta}\frac{\partial \boldsymbol{q}}{\partial r_\alpha} \quad (\alpha = 1, \ldots, N)\,, \tag{34}$$

$$\left\{\frac{\partial \boldsymbol{\phi}}{\partial \theta} - \frac{1}{\theta}\frac{\partial \boldsymbol{q}}{\partial \theta}\right\} \cdot \boldsymbol{g} \geq 0. \tag{35}$$

The simplest possibility to fulfil this set of conditions is the choice of the heat flux according to Fourier's heat conduction model

$$\boldsymbol{q} = -\lambda \operatorname{grad} \theta, \tag{36}$$

where λ is the heat conductivity, and the entropy flux

$$\boldsymbol{\phi} = \frac{1}{\theta}\boldsymbol{q}, \tag{37}$$

which is often assumed a priori. However, this issue will not be discussed in the following. After having specified the free energy, we will evaluate the inequality (30) in the form

$$-\left\{\rho\frac{\partial \psi}{\partial r_\alpha} + \theta\lambda^V A_\alpha\right\}\dot{r}_\alpha \geq 0 \quad (\alpha = 1, \ldots, N) \tag{38}$$

to find evolution equations for the grain radii. Then, as a last step, the remaining Lagrange multiplier λ^V will have to be determined by evaluating the condition of volume conservation, (21).

3.2. Free Energy and Evolution Equations

The energy stored in the boundary of an individual grain can be expressed by the product of the grain boundary energy per unit area σ_α and its surface area. Then, the sum of the contributions of all N grains provides the total stored grain boundary energy. In addition, the free energy may depend on a caloric function $C(\theta)$, which will be defined later, such that

$$\rho\psi = \frac{1}{2V}\sum_{\alpha=1}^{N}\sigma_\alpha A_\alpha + C(\theta). \tag{39}$$

Note that in (39), the factor $1/2$ compensates the fact that each boundary is associated with two grains and is therefore counted twice. Insertion into (38) yields, for a three-dimensional problem with spherical grains,

$$-\frac{A_\alpha}{V}\left\{\frac{\sigma_\alpha}{r_\alpha} + \Lambda\right\}\dot{r}_\alpha \geq 0 \quad (\alpha = 1, \ldots, N) \tag{40}$$

where the abbreviation $\Lambda = \theta\lambda^V V$ is introduced. Usually, the grain boundary velocity is assumed to be proportional to a driving force. This motivates to identify

$$p_\alpha = -\left(\frac{\sigma_\alpha}{r_\alpha} + \Lambda\right) \quad (\alpha = 1, \ldots, N) \tag{41}$$

in (40) as the driving forces for grain boundary motion which, multiplied by the mobilities M_α, determine the respective grain radius evolution,

$$\dot{r}_\alpha = M_\alpha p_\alpha \quad (\alpha = 1, \dots, N)\,. \tag{42}$$

In order to check that our choice of the constitutive quantities leads to a non-negative entropy production, we calculate the total dissipation rate in the system. Adding up all contributions of (30) and (31) and inserting our grain growth model as well as the heat and entropy flux vectors leads to

$$\begin{aligned}\rho\theta\gamma &= -\sum_{\alpha=1}^{N}\left\{\rho\frac{\partial\psi}{\partial r_\alpha} + \theta\lambda^V A_\alpha\right\}\dot{r}_\alpha + \left\{\theta\frac{\partial\boldsymbol{\phi}}{\partial\theta} - \frac{\partial\boldsymbol{q}}{\partial\theta}\right\}\cdot\operatorname{grad}\theta \\ &= \sum_{\alpha=1}^{N}\frac{A_\alpha}{V}M_\alpha p_\alpha^2 + \frac{\lambda}{\theta}\left(\operatorname{grad}\theta\right)^2 \geq 0.\end{aligned} \tag{43}$$

Since the material parameters M_α and λ are positive, this inequality is always fulfilled.

As a next step, the Lagrange multiplier Λ is calculated. Therefore, the evolution equations (42) are inserted into the condition of volume conservation, (21), yielding the condition

$$4\pi\sum_{\alpha=1}^{N} r_\alpha^2\dot{r}_\alpha = -4\pi\sum_{\alpha=1}^{N} M_\alpha\left(\sigma_\alpha r_\alpha + \Lambda r_\alpha^2\right) = 0. \tag{44}$$

Consequently, the Lagrange multiplier is

$$\Lambda = -\frac{\sum_{\alpha=1}^{N} M_\alpha\sigma_\alpha r_\alpha}{\sum_{\alpha=1}^{N} M_\alpha r_\alpha^2}. \tag{45}$$

To describe the growth of cylindrical grains in a thin film, we neglect the energy of free surfaces and take only the grain boundary energy into account. The problem can thus be considered as two-dimensional. The free energy is expressed by (39) with $A_\alpha = 2\pi r_\alpha h$ and we obtain, analogously to (40),

$$-\frac{A_\alpha}{V}\left\{\frac{\sigma_\alpha}{2r_\alpha} + \Lambda\right\}\dot{r}_\alpha \geq 0 \quad (\alpha = 1, \dots, N)\,. \tag{46}$$

The driving forces are identified by

$$p_\alpha = -\left(\frac{\sigma_\alpha}{2r_\alpha} + \Lambda\right) \quad (\alpha = 1, \dots, N)\,, \tag{47}$$

such that the Lagrange multiplier is, due to (22),

$$\Lambda = -\frac{\sum_{\alpha=1}^{N} M_\alpha\sigma_\alpha}{2\sum_{\alpha=1}^{N} M_\alpha r_\alpha}. \tag{48}$$

The temperature dependence of the grain boundary mobility is commonly described by the Arrhenius approach

$$M_\alpha = M_{0,\alpha}\exp\left(-\frac{Q_\alpha}{R\theta}\right) \quad (\alpha = 1, \dots, N)\,. \tag{49}$$

In this relation, $M_{0,\alpha}$ is a constant mobility factor, Q_α is the activation energy for the motion of the boundary of grain α and R is the gas constant.

For the caloric function, we recall the definition of the specific heat capacity at constant deformation,

$$c_{\mathrm{d}} = -\theta \frac{\partial^2 \psi}{\partial \theta^2} = -\frac{\theta}{\rho} \frac{\partial^2 C(\theta)}{\partial \theta^2}. \tag{50}$$

If we assume c_{d} to be constant, integration of (50) yields

$$C(\theta) = \rho c_{\mathrm{d}} \left[(\theta - \theta_0) - \theta \ln \frac{\theta}{\theta_0} \right] \tag{51}$$

with a reference temperature θ_0. The essential components of the grain growth model are summarised in table 1.

Table 1. Summary of the grain growth model.

Free Energy	$\rho\psi = \frac{1}{2V} \sum\limits_{\alpha=1}^{N} \sigma_\alpha A_\alpha + \rho c_{\mathrm{d}} \left[(\theta - \theta_0) - \theta \ln \frac{\theta}{\theta_0} \right]$	
Grain Radius Evolution	$\dot{r}_\alpha = M_\alpha p_\alpha \quad (\alpha = 1, \ldots, N)$	
Mobility	$M_\alpha = M_{0,\alpha} \exp\left(-\frac{Q_\alpha}{R\theta} \right)$	
Effective Surface	3D: $A_\alpha = 4\pi r_\alpha^2$	2D: $A_\alpha = 2\pi r_\alpha h$
Driving Force	3D: $p_\alpha = -\left[\frac{\sigma_\alpha}{r_\alpha} - \frac{\sum\limits_{\beta=1}^{N} M_\beta \sigma_\beta r_\beta}{\sum\limits_{\beta=1}^{N} M_\beta r_\beta^2} \right]$	2D: $p_\alpha = -\frac{1}{2}\left[\frac{\sigma_\alpha}{r_\alpha} - \frac{\sum\limits_{\beta=1}^{N} M_\beta \sigma_\beta}{\sum\limits_{\beta=1}^{N} M_\beta r_\beta} \right]$

4. Discussion and Application

4.1. Remark on Rational Thermodynamics

In section 2, we used the concept of Rational Extended Thermodynamics (RET) by Müller and Liu instead of classical Rational Thermodynamics (RT) by Coleman an Noll, whereas the latter is the more common approach in continuum mechanics. If alternatively we had used RT, a modification of the standard procedure would have been necessary. From the dependence of the free energy on internal variables, say on the grain radii $\{r_\alpha\}$, the common form of the Clausius-Duhem inequality immediately yields $\dot{r}_\alpha \propto -\rho\, \partial\psi / \partial r_\alpha$, such that the driving forces should simply be $p_\alpha = -\sigma_\alpha / r_\alpha$ $(\alpha = 1, \ldots, N)$. In this case, however, all grains would shrink and vanish. Obviously, it is necessary to include the condition of volume conservation (21) to obtain a meaningful result. This can be done by appending the side condition with a Lagrange multiplier to the Clausius-Duhem inequality. On the other hand, it is more consistent to treat all balance equations in the same way as suggested by Liu. In summary, RET offers the flexibility to incorporate additional balance equations and overcomes the problematic aspects of RT discussed in section 1.

4.2. Comparison to Existing Grain Growth Models

Although we obtained our model by a novel procedure, it can be easily found that it is similar to well established concepts. We can reformulate (42) for both three- and two-dimensional problems as

$$\dot{r}_\alpha = cM_\alpha\sigma_\alpha\left(\frac{1}{r_{\mathrm{cr},\alpha}} - \frac{1}{r_\alpha}\right) \quad (\alpha = 1,\ldots,N) \tag{52}$$

by defining the critical radii $r_{\mathrm{cr},\alpha}$. The critical radius is different for individual grains only if individual values of the specific grain boundary energy are assumed. In this case, the larger σ_α is compared to the values of the other grains the larger is $r_{\mathrm{cr},\alpha}$. Otherwise, the critical radius is identical for all grains. In three dimensions, we have $c = 1$ and

$$r_{\mathrm{cr},\alpha} = \frac{\sum_{\beta=1}^{N} M_\beta r_\beta^2}{\sum_{\beta=1}^{N} M_\beta \frac{\sigma_\beta}{\sigma_\alpha} r_\beta} \quad (\alpha = 1,\ldots,N)\,, \tag{53}$$

whereas in two dimensions $c = 1/2$ and

$$r_{\mathrm{cr},\alpha} = \frac{\sum_{\beta=1}^{N} M_\beta r_\beta}{\sum_{\beta=1}^{N} M_\beta \frac{\sigma_\beta}{\sigma_\alpha}} \quad (\alpha = 1,\ldots,N)\,. \tag{54}$$

Comparing (52) to (3), it becomes obvious that our growth equation exactly matches that by Fischer et al. [32] apart from the fact that their constant c has twice the value of ours. Since we make exactly the same assumption for the stored energy, the difference arises from the different thermodynamic principles. Compared to Hillert's model, (2), the only difference is a more complex definition of the critical radii. However, all definitions show a noticeable similarity which becomes particularly obvious if all grain boundaries have the same mobility and specific energy. Then, we obtain from (52)

$$\dot{r}_\alpha = cM\sigma\left(\frac{1}{r_{\mathrm{cr}}} - \frac{1}{r_\alpha}\right), \tag{55}$$

in which the critical radius is unique. In two dimensions, it simplifies to

$$r_{\mathrm{cr}} = \frac{1}{N}\sum_{\alpha=1}^{N} r_\alpha = \overline{r}, \tag{56}$$

which is exactly the result obtained by Hillert [16]. In the three-dimensional case, the critical radius is

$$r_{\mathrm{cr}} = \frac{\sum_{\alpha=1}^{N} r_\alpha^2}{\sum_{\alpha=1}^{N} r_\alpha} = \frac{r_{\mathrm{rms}}^2}{\overline{r}} \tag{57}$$

with the root mean square radius

$$r_{\mathrm{rms}} = \sqrt{\frac{1}{N}\sum_{\alpha=1}^{N} r_\alpha^2}. \tag{58}$$

In table 2, the definitions of c and the critical radii of the three models are compared.

It is worth to consider an even more specific case of three-dimensional grain growth. If the system is initialised with grain sizes according to Hillert's distribution [16], then

Table 2. Comparison of the present model to those by Hillert [16] and Fischer et al. [32] assuming identical properties for all grains.

Dimensionality	2D		3D	
	c	r_{cr}	c	r_{cr}
Hillert	1/2	$\overline{r}$	1	$9/8\ \overline{r}$
Fischer et al.	1	$\overline{r}$	2	$r_{\mathrm{rms}}^2/\overline{r}$
Present Work	1/2	$\overline{r}$	1	$r_{\mathrm{rms}}^2/\overline{r}$

at all times during evolution, the grain sizes can be described by Hillert's distribution and the critical radius of our model and that by Fischer et al. turns into that found by Hillert,

$$r_{\mathrm{cr}} = \frac{\sum_{\alpha=1}^{N} r_\alpha^2}{\sum_{\alpha=1}^{N} r_\alpha} = \frac{9}{8}\overline{r}. \tag{59}$$

This means that our model is actually a thermodynamic extension of Hillert's one to systems in which the grains may have individual properties. Its great benefit is the unified thermodynamic framework from which it has been derived and which provides the possibility to incorporate thermomechanics and further microstructural phenomena like recrystallization.

4.3. Application to Grain Growth in Copper

We used our model to simulate grain growth in pure copper with MATLAB and compared the results to experiments from literature. For the boundary energy of all grains, a constant value $\sigma = 0.625\,\mathrm{J/m^2}$ is assumed, which has been proposed for copper in [35, p. 129]. The pre-exponential mobility factor M_0 and the activation energy Q are assumed to be equal for all grains, too. Their values have to be determined individually for each reference. For visualisation, the mean grain radius is calculated from the individual radii at each time. Since during the system evolution the number of grains decreases, statistical quantities such as the mean size gradually become less meaningful. The initial number of grains has thus to be chosen sufficiently large. The mean radius evolves discontinuously, because it jumps each time one grain vanishes.

Lian et al. [36] used strongly cold worked copper of 99.98 % purity to study grain growth at 200 °C. Increasing from 0.16 µm to 1.28 µm, the reported mean grain diameter is small enough to assume that surface effects can be neglected. Lian et al. found an activation energy of $Q = 102\,\mathrm{kJ/mol}$. Using this value, we can very accurately reproduce the experimental results with the mobility factor $M_0 = 9.0 \cdot 10^{-5}\,\mathrm{m^4/(J\,s)}$ if the system is initialised with Hillert's distribution [16]. The results for an initial number of 3000 grains are shown in figure 1. However, there is no evidence by the authors that recrystallization had been completed before their measurement. Grain boundary energy driven grain growth may thus be superimposed by recrystallization in the first seconds.

Ghauri et al. [37] investigated grain growth in hard-drawn 99.999 % purity copper wires. The wire diameter was 3 mm and the mean grain diameter increased from 10 µm to 184 µm at the highest temperature. Surface effects can thus be neglected. With the value $Q = 82\,\mathrm{kJ/mol}$ given by Ghauri et al., the measured sizes are well represented by our model using $M_0 = 3.5 \cdot 10^{-8}\,\mathrm{m^4/(J\,s)}$ if the system is initialised with Hillert's distribution for three dimensions. Figure 2 shows the results for an initial number of 10 000 grains. Again, we cannot exclude that additional recrystallization occurred in an early stage of the experiment. The fact that experimental data is available at four annealing temperatures demonstrates the predictive power of the model. Actually, it is sufficient to fit the mobility parameter using only one temperature, such that the results at the remaining temperatures can be accurately calculated.

Gangulee [38] investigated grain growth in thin electroplated copper films on oxidised silicon substrates at three annealing temperatures. Since mean grain diameters up to 4.7 µm are reported whereas the film thickness is only 1.1 µm, the problem has to be considered as two-dimensional according to the arguments in section 3. The specimens had been pre-annealed to separate the preceding recrystallization from grain boundary energy driven grain growth. With $Q = 154\,\mathrm{kJ/mol}$ given by Gangulee, we can reproduce the experimental results with Hillert's distribution for two dimensions and $M_0 = 5.6 \cdot 10^{-4}\,\mathrm{m^4/(J\,s)}$. Figure 3 shows the results for an initial number of 1000 grains.

4.4. Implications on the Energy Balance

An major benefit of thermodynamic approaches, as introduced before, is the fact that coupling phenomena are already represented without further modifications. In order to demonstrate the energy effects of our grain growth model, we simulate a calorimetry

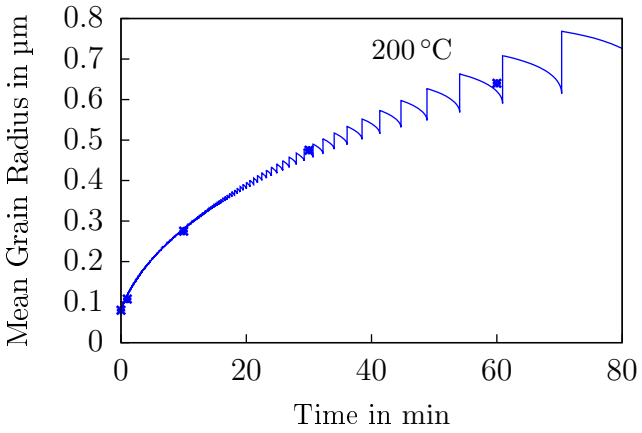

Figure 1. Mean radius evolution for 3000 grains with Hillert's distribution, $\sigma = 0.625\,\mathrm{J/m^2}$, $Q = 102\,\mathrm{kJ/mol}$, $M_0 = 9.0 \cdot 10^{-5}\,\mathrm{m^4/(J\,s)}$. Experimental data from [36].

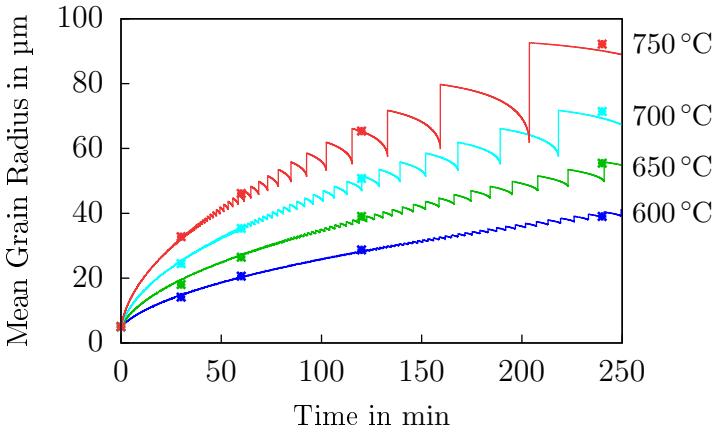

Figure 2. Mean radius evolution for 10 000 grains with Hillert's distribution, $\sigma = 0.625\,\mathrm{J/m^2}$, $Q = 82\,\mathrm{kJ/mol}$, $M_0 = 3.5 \cdot 10^{-8}\,\mathrm{m^4/(J\,s)}$. Experimental data from [37].

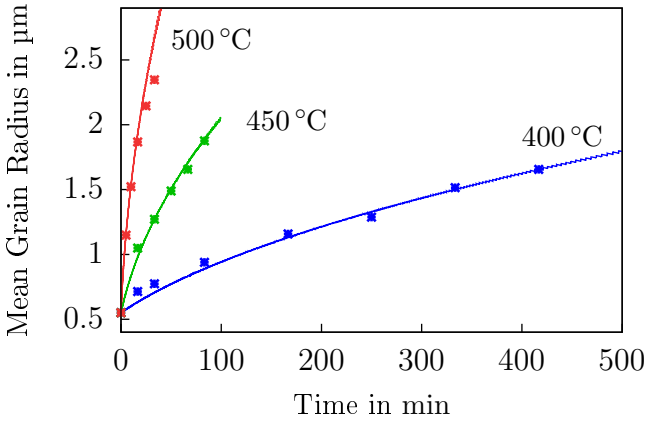

Figure 3. Mean radius evolution for 1000 two-dimensional grains with Hillert's distribution for two dimensions with $\sigma = 0.625\,\mathrm{J/m^2}$, $Q = 154\,\mathrm{kJ/mol}$, $M_0 = 5.6 \cdot 10^{-4}\,\mathrm{m^4/(J\,s)}$. Experimental data from [38].

experiment in which a specimen is heated with a predefined constant heating rate $\dot{\theta}$ by controlling the heat supply w. From (20) we know that the heat supply is equal to the change of internal energy,

$$w = -\frac{1}{\rho}\operatorname{div} \boldsymbol{q} = \dot{e}. \tag{60}$$

On the other hand, using our approach (39) for the free energy and due to (32), the change of the free energy is

$$\dot{e} = \dot{\psi} + \theta\dot{\eta} + \eta\dot{\theta} = -\theta\frac{\partial^2\psi}{\partial\theta^2}\dot{\theta} + \sum_{\alpha=1}^{N}\frac{\partial\psi}{\partial r_\alpha}\dot{r}_\alpha. \tag{61}$$

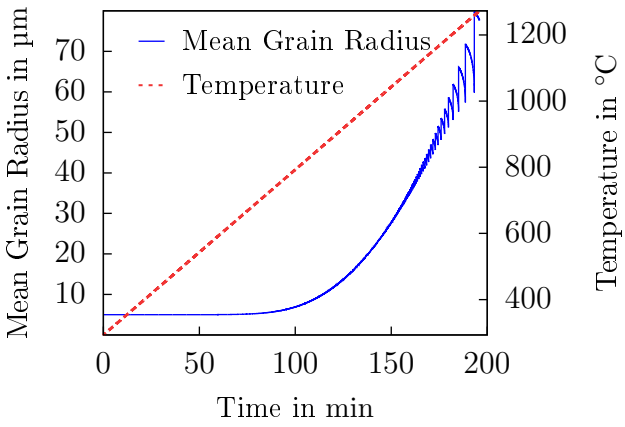

Figure 4. Temperature ramp applied in the virtual calorimetry experiment and resulting evolution of the mean grain size.

Therefore, the heat supply can be expressed by

$$w = c_{\mathrm{d}}\dot{\theta} + \sum_{\alpha=1}^{N} \frac{\partial \psi}{\partial r_\alpha}\dot{r}_\alpha, \tag{62}$$

where the definition of the specific heat capacity according to (50) is used. Real experiments are usually performed under atmospheric thus constant pressure. Therefore, in the strict sense, we should use the heat capacity at constant stress for our virtual experiment. However, as by definition of our problem no deformation occurs, it is natural to use the heat capacity at constant deformation. We use the value $c_{\mathrm{d}} = 390\,\mathrm{J/(kg\,K)}$ as a reasonable mean value within a large temperature range above ambient temperature [39].

In (62), we can distinguish one contribution of the heat supply related to increasing the temperature and one related to the change of grain boundary energy. The former is positive whereas the latter is negative because the system aims to reduce its energy by the growth of larger grains at the expense of smaller ones. Consequently, this contribution reduces the heat supply needed to achieve the desired heating rate. We used the model parameters determined to reproduce the results by Ghauri et al. [37] and applied a heating rate $\dot{\theta} = 5\,\mathrm{K/min}$. Figure 4 shows how the mean grain radius evolves due to the temperature ramp.

In figure 5, the two contributions to the heat supply, $c_{\mathrm{d}}\dot{\theta}$ and that by grain boundary (GB) energy release, are compared. Whereas the former is constant, the latter initially increases with increasing temperature and then decreases forming a distinct peak. Such peaks are commonly observed in real calorimetry experiments when changes of the microstructure or phase transitions occur.

We emphasise that the decrease of the grain growth contribution does not arise due to the limited system size. It can rather be explained by the fact that in an advanced stage of grain growth, the ratio of grain boundary surface and volume reduces drastically,

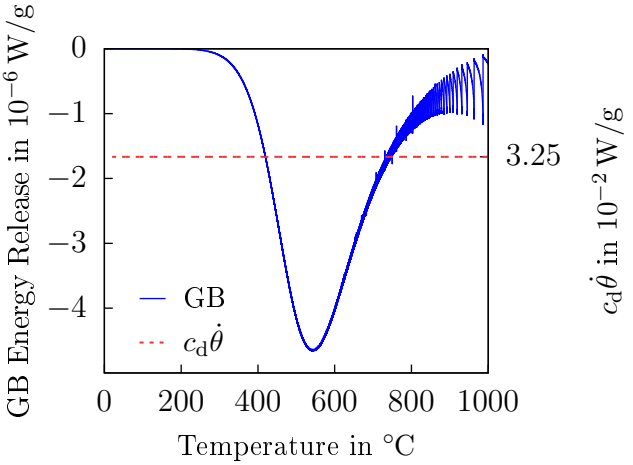

Figure 5. Comparison of the two contributions to the heat supply in the virtual calorimetry experiment. Note the opposed signs and different orders of magnitude.

independently of the total system size. However, by comparing the orders of magnitude of both contributions, it becomes obvious that in a real measurement, the effect of grain growth to the calorimetry signal will be very small.

5. Conclusions

We revisited Liu's entropy principle [8] and prepared it for deriving thermodynamically consistent thermomechanical constitutive equations taking the microstructure of the material into account. Besides classical quantities of continuum mechanics and thermodynamics, unconstrained internal variables as well as variables subject to further side conditions can be incorporated into the present framework. After having introduced some simplifications, we demonstrated the applicability of the principle by deriving a grain growth model in which the grain sizes are a set of constrained internal variables. Although we used a novel approach to grain growth, our model is similar to existing and well established concepts. It is shown that it is an extension of Hillert's model [16] to more general systems embedded in a consistent thermodynamic framework. The model is suitable to reproduce experimental results very accurately. Finally, by taking a caloric function in the free energy into account, we studied the implications of grain growth on the energy balance.

The present modelling approach closely connects the classical quantities of continuum thermomechanics and the microstructure through the enhanced entropy balance. In that, it overcomes the problem in Rational Thermodynamics to deal with constraints on the internal variables. Therefore, it is appropriate for a straightforward extension to thermoelasticity and thermoplasticity considering the microstructure, which we aim to realise in our future work. In addition, we plan to include recrystallization as a further mechanism. Even precipitates might be considered in terms of an additional set of constrained variables if the chemical composition is incorporated.

Acknowledgements

The funding by Deutsche Forschungsgemeinschaft under the reference number HE 3096/7-1 within the Priority Programme 1713 "Strong Coupling of Thermo-Chemical and Thermo-Mechanical States in Applied Materials" is gratefully acknowledged.

References

[1] Jou D, Casas-Vázquez J and Lebon G 2010 *Extended Irreversible Thermodynamics* 4th ed (New York: Springer) ISBN 978-90-481-3073-3
[2] Onsager L 1931 *Phys. Rev.* **37** 405–426
[3] Onsager L 1931 *Phys. Rev.* **38** 2265–2279
[4] Coleman B D and Truesdell C 1960 *J. Chem. Phys.* **33** 28–31
[5] Coleman B D and Noll W 1963 *Arch. Ration. Mech. An.* **13** 167–178
[6] Müller I and Ruggeri T 1998 *Rational Extended Thermodynamics* 2nd ed (New York, Berlin, Heidelberg: Springer) ISBN 0-387-98373-2
[7] Müller I 1971 *Arch. Ration. Mech. An.* **41** 319–332
[8] Liu I S 1972 *Arch. Ration. Mech. An.* **46** 131–148
[9] Müller I 1973 *Z. Naturforsch. A* **28** 1801–1813
[10] Svendsen B and Hutter K 1995 *Int. J. Eng. Sci* **33** 2021–2054 ISSN 00207225
[11] Burke J E and Turnbull D 1952 *Prog. Met. Phys.* **3** 220–292
[12] Feltham P 1957 *Acta Metall. Mater.* **5** 97–105 ISSN 00016160
[13] von Neumann J 1952 *Metal Interfaces* ed Herring C (Cleveland: American Society of Metals) pp 108–110
[14] Mullins W W 1956 *J. Appl. Phys.* **27** 900–904
[15] Lifshitz I M and Slyozov V V 1958 *J. Exp. Theor. Phys.* **35** 479
[16] Hillert M 1965 *Acta Metall. Mater.* **13** 227–238 ISSN 00016160
[17] Rios P R and Glicksman M E 2004 *Scripta Mater.* **51** 629–633 ISSN 13596462
[18] Rios P R and Glicksman M E 2006 *Acta Mater.* **54** 1041–1051 ISSN 13596454
[19] Radhakrishnan B and Zacharia T 1995 *Metall. Mater. Trans. A* **26** 167–180
[20] Zöllner D and Streitenberger P 2006 *Scripta Mater.* **54** 1697–1702 ISSN 13596462
[21] Weygand D, Bréchet Y, Lépinoux J and Gust W 1999 *Philos. Mag. B* **79** 703–716
[22] Wakai F, Enomoto N and Ogawa H 2000 *Acta Mater.* **48** 1297–1311 ISSN 13596454
[23] Raabe D and Becker R C 2000 *Model. Simul. Mater. Sc.* **8** 445–462
[24] Raghavan S and Sahay S S 2007 *Mat. Sci. Eng. A* **445-446** 203–209 ISSN 09215093
[25] Fan D and Chen L Q 1997 *Acta Mater.* **45** 611–622 ISSN 13596454
[26] Darvishi Kamachali R and Steinbach I 2012 *Acta Mater.* **60** 2719–2728 ISSN 13596454
[27] Gruber J, Ma N, Wang Y, Rollett A D and Rohrer G S 2006 *Model. Simul. Mater. Sc.* **14** 1189–1195
[28] Darvishi Kamachali R, Abbondandolo A, Siburg K F and Steinbach I 2015 *Acta Mater.* **90** 252–258 ISSN 13596454
[29] Payton E J, Wang G, Mills M J and Wang Y 2013 *Acta Mater.* **61** 1316–1326 ISSN 13596454
[30] Rios P R, Gottstein G and Shvindlerman L S 2002 *Mater. Sci. Eng. A* **332** 231–235 ISSN 09215093
[31] Berdichevsky V L 2012 *Int. J. Eng. Sci* **57** 50–78 ISSN 00207225
[32] Fischer F D, Svoboda J and Fratzl P 2003 *Philos. Mag.* **83** 1075–1093 ISSN 1478-6435
[33] Coleman B D and Gurtin M E 1967 *J. Chem. Phys.* **47** 597–613
[34] Truesdell C and Noll W 1965 The Non-Linear Field Theories of Mechanics *Handbuch der Physik* ed Flügge S (Berlin, Heidelberg, New York: Springer)
[35] Humphreys F J and Hatherly M 2004 *Recrystallization and Related Annealing Phenomena* 2nd ed (Oxford: Elsevier) ISBN 0-08-044164-5
[36] Lian J, Valiev R Z and Baudelet B 1995 *Acta Metall. Mater.* **43** 4165–4170 ISSN 09567151

[37] Ghauri I M, Butt M Z and Raza S M 1990 *J. Mater. Sci.* **25** 4782–4784
[38] Gangulee A 1974 *J. Appl. Phys.* **45** 3749–3756
[39] White G K and Collocott S J 1984 *J. Phys. Chem. Ref. Data* **13** 1251–1257